

Electronic Supporting Information

A Zn²⁺-coordinated boronate dipyrin as a chemodosimeter toward hydrogen peroxide

Kaori Sakakibara, Yuki Takahashi, Ryuhei Nishiyabu and Yuji Kubo*

Department of Applied Chemistry, Graduate School of Urban Environmental Sciences, Tokyo Metropolitan University, 1-1 Minami-ohsawa, Hachioji, Tokyo 192-0397, Japan
E-mail; yujik@tmu.ac.jp

Table of contents

Fig. S1 Change in the absorbance spectra of 1 upon adding incremental amount of Zn(OAc) ₂ in EtOH.	SI-2
Fig. S2 ESI-MS spectra of the EtOH solution of 1 in the presence of 3 equiv. of Zn (OAc) ₂ .	SI-2
Fig. S3 FAB-MS spectra of solid isolated from the EtOH solution of 1 and Zn(OAc) ₂ .	SI-3
Fig. S4 Time-course analysis of absorption spectra of Zn-12 after adding H ₂ O ₂ in EtOH/CHCl ₃ (1:1 v/v).	SI-3
Fig. S5 Change in absorption intensity of 1 at 581 nm and 597 nm as a function of time in the presence of Zn(OAc) ₂ after adding an excess amount of H ₂ O ₂ in EtOH.	SI-4
Fig. S6 ESI-MS spectra of the EtOH solution of 1 and Zn(OAc) ₂ in 12 h after adding of H ₂ O ₂ in EtOH.	SI-4
Fig. S7 ESI-MS spectra of the EtOH solution of 1 in the presence of 3 equiv. of Zn (OAc) ₂ when 5 hours passed after adding H ₂ O ₂ .	SI-5
Fig. S8 Time-dependent change in absorption intensity of 1 with Zn(OAc) ₂ by adding H ₂ O ₂ in the presence of TBAOH.	SI-5
Fig. S9 A plot of a change in absorption intensity of 1 in the presence of Zn(OAc) ₂ as a function of H ₂ O ₂ concentration added in EtOH.	SI-6
Fig. S10 A plot of a change in fluorescence intensity of 1 in the presence of Zn(OAc) ₂ as a function of H ₂ O ₂ concentration added in EtOH.	SI-6
Fig. S11 Colorimetric response of 1 and Zn ²⁺ -coated filter paper exposed to varying amounts of H ₂ O ₂ vapor.	S1-7
Fig. S12 ¹³ C NMR spectrum of 1 in CDCl ₃ .	SI-7
Fig. S13 ¹³ C NMR spectrum of 1 in CDCl ₃ .	SI-8
Fig. S14 FAB-MS spectrum of 1 .	SI-8

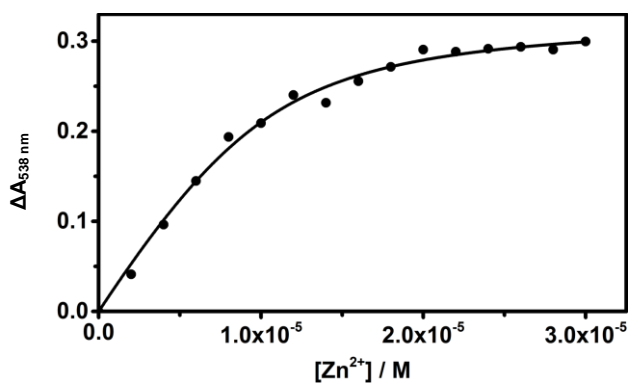


Fig. S1. Change in the absorbance of **1** at 538 nm upon adding incremental amount of Zn(OAc)₂ in EtOH. The data was acquired in 5 min after treating with Zn(OAc)₂.

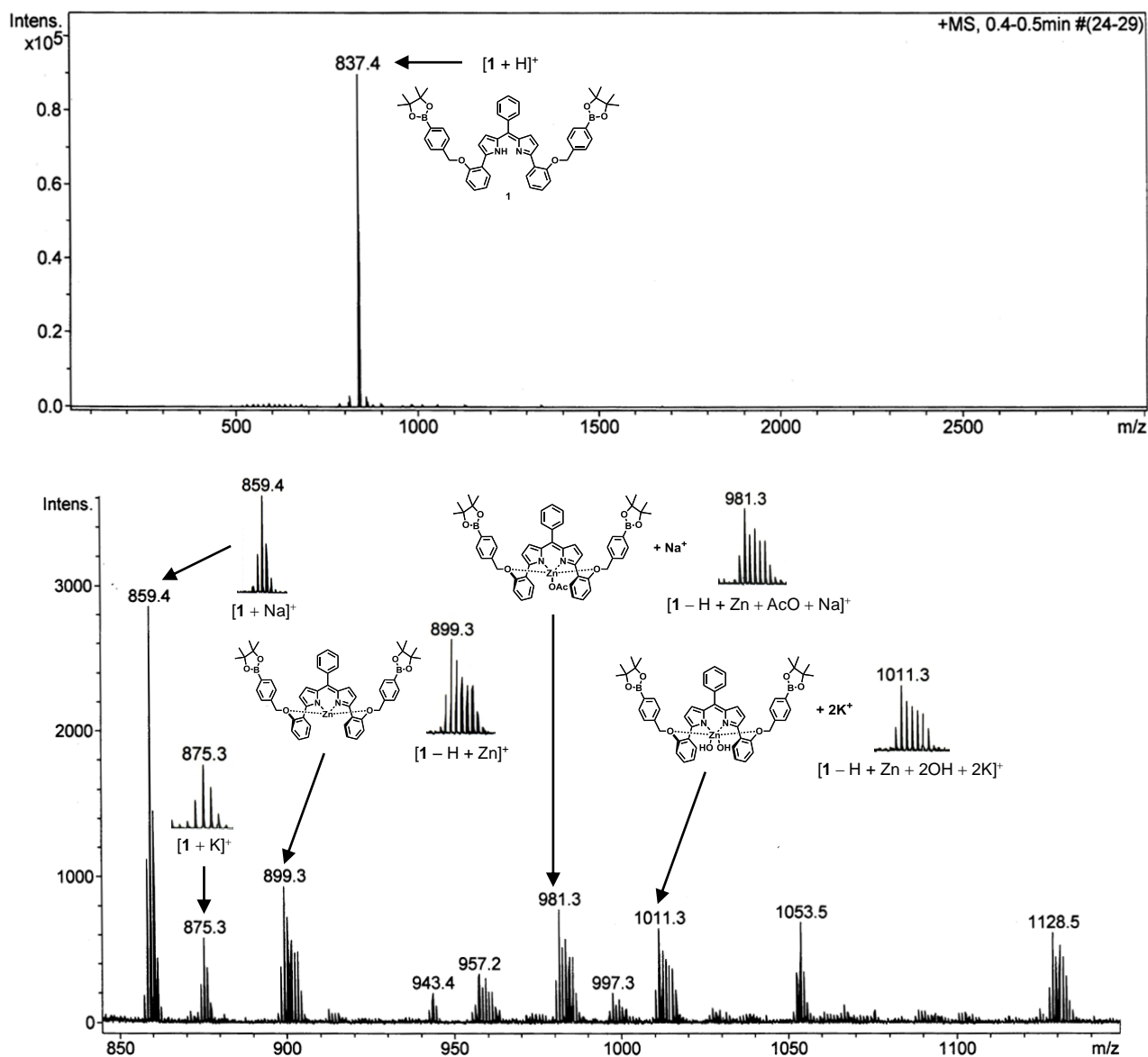


Fig. S2. ESI-MS spectra in the positive mode of the EtOH solution of **1** in the presence of 3 equiv. of Zn(OAc)₂. The data were acquired in 5 min at 100 °C.

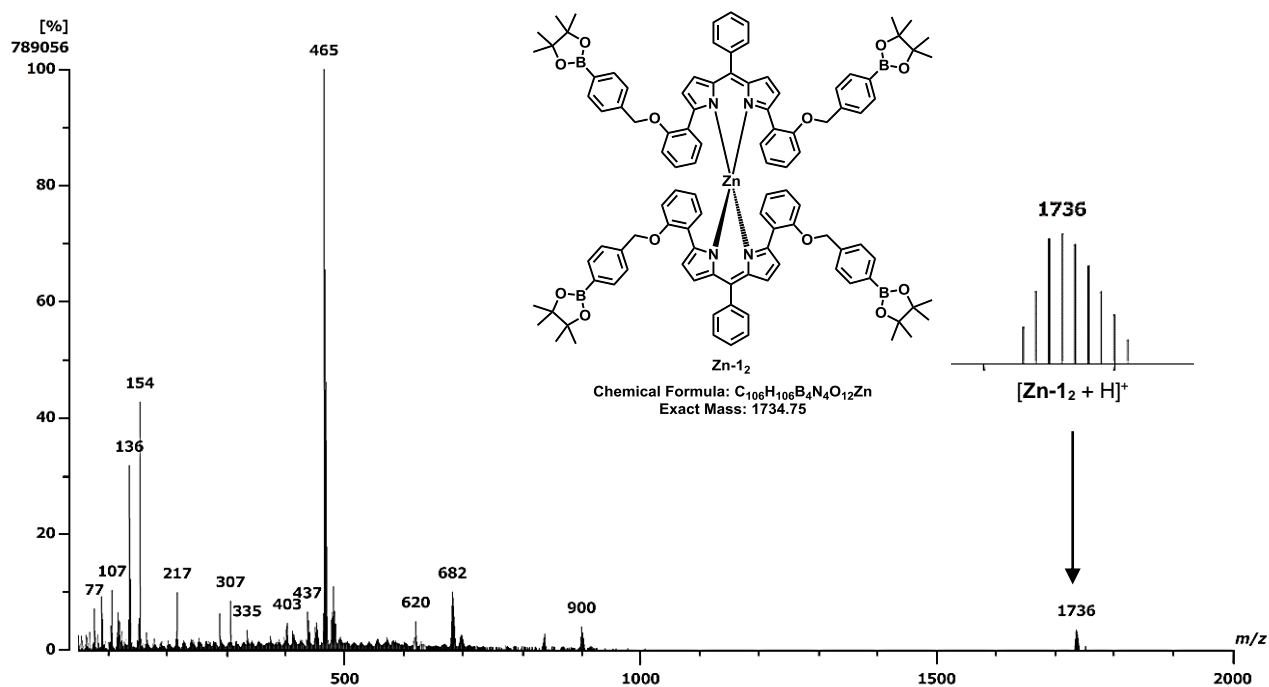


Fig. S3. FAB-MS spectra of solid isolated from the evaporation of EtOH solution where **1** (50 μmol) and $Zn(OAc)_2$ (50 μmol) were dissolved. (The plausible structure of **Zn-12** has shown).

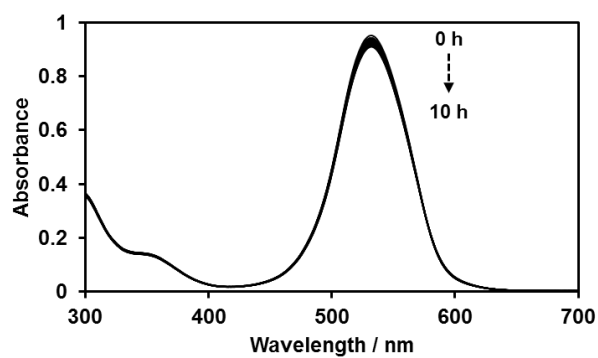


Fig. S4. Time-course analysis of absorption spectra of **Zn-12** (10 μM) as a plausible complex after adding H_2O_2 (1mM) in EtOH/ $CHCl_3$ (1:1 v/v).

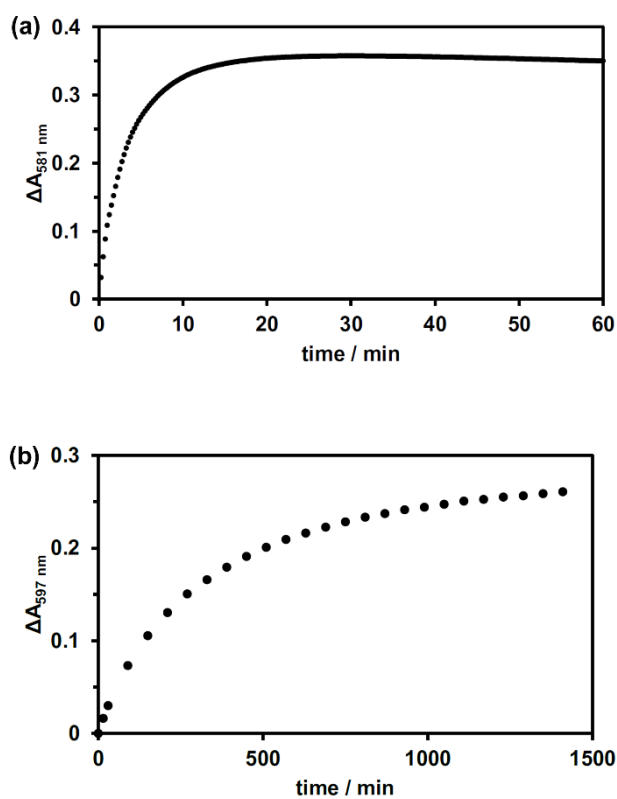


Fig. S5. Change in absorption intensity of **1** at 581 nm (a) and 597 nm (b) as a function of time in the presence of 3 equiv. of $\text{Zn}(\text{OAc})_2$ after adding an excess amount of H_2O_2 (1 mM) in EtOH at 25 °C.

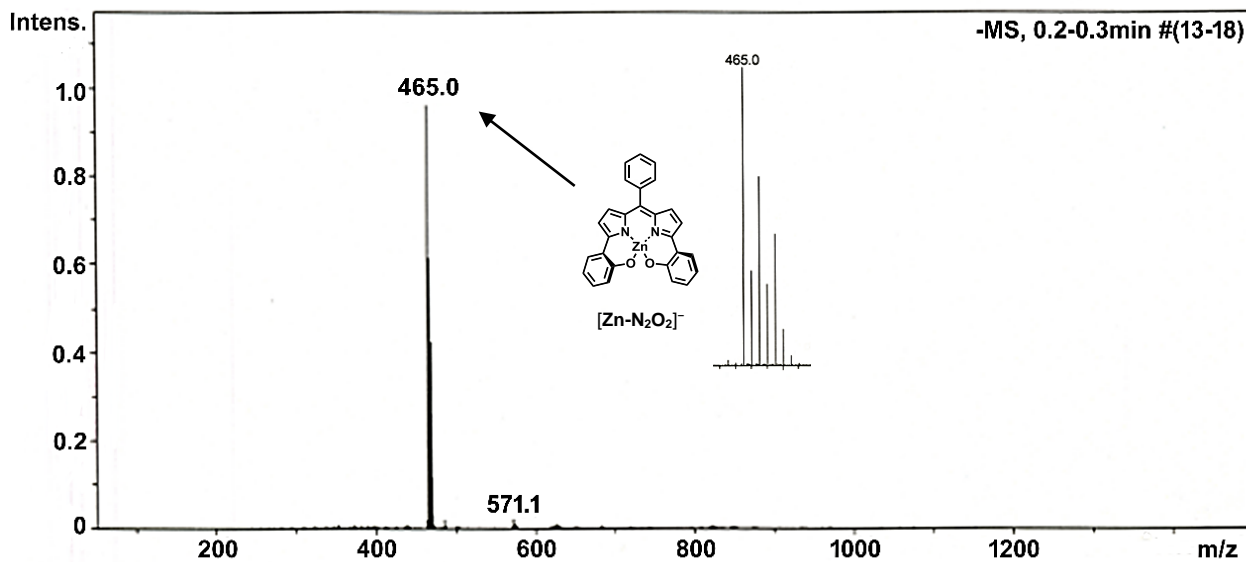


Fig. S6. ESI-MS spectra in the negative mode of the EtOH solution of **1** (10 μM) and $\text{Zn}(\text{OAc})_2$ (30 μM) in 12 h after adding of H_2O_2 in EtOH.

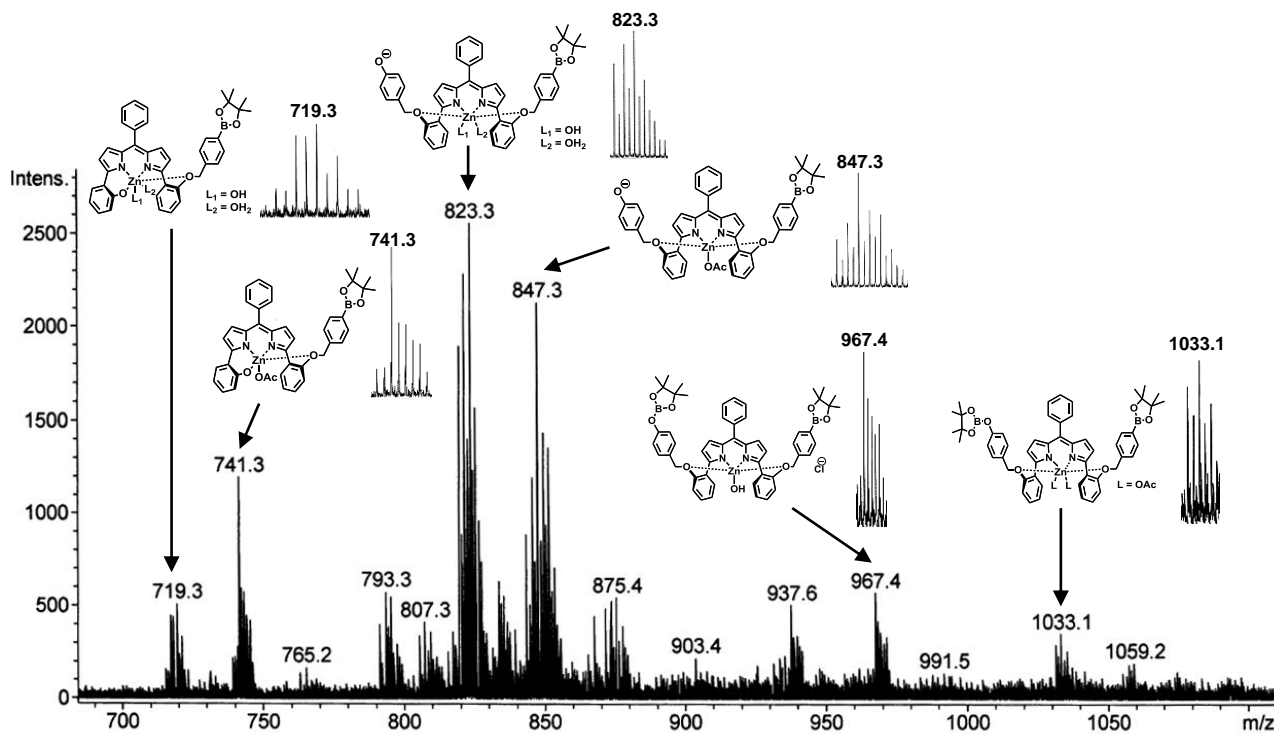


Fig. S7. ESI-MS spectra in the negative mode at 100 °C of the EtOH solution of **1** in the presence of 3 equiv. of Zn (OAc)₂ when 5 hours passed after adding H₂O₂.

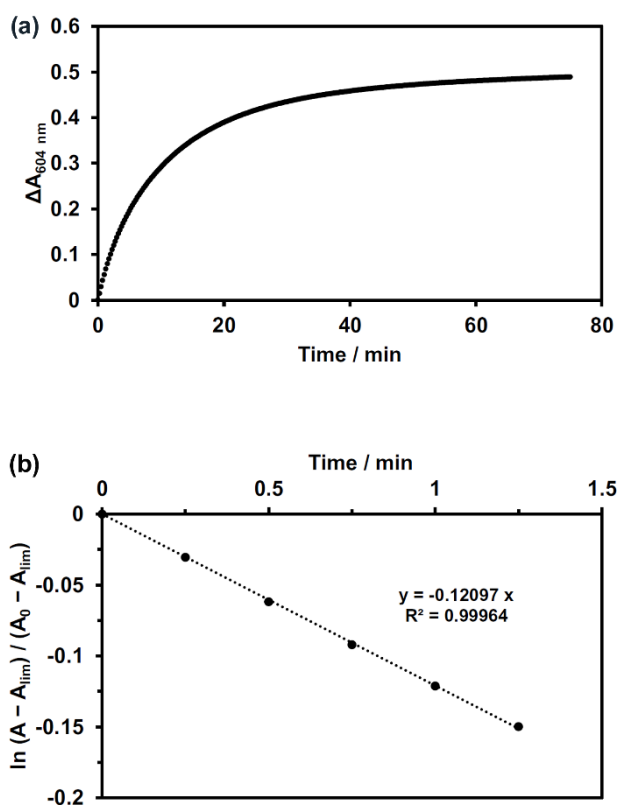


Fig. S8. (a) Time-dependent change in absorption band of **1** (10 μM) with Zn(OAc)₂ (30 μM) by adding H₂O₂ (50 μM) in the presence of TBAOH (1 mM). (b) A plot of $\ln(A - A_{lim}) / (A_0 - A_{lim})$ as a function of time.

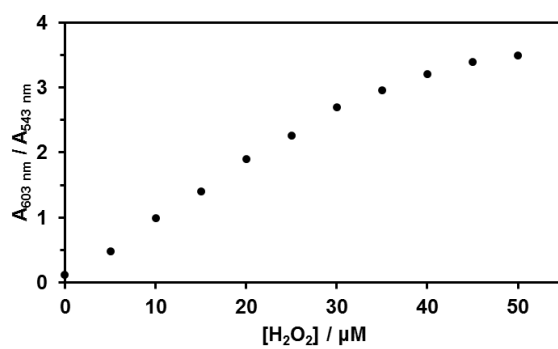


Fig. S9. A plot of a change in absorption intensity of **1** (10 μM) in the presence of Zn(OAc)₂ (30 μM) as a function of H₂O₂ concentration added in EtOH at 25 °C. The data were acquired in 30 min after adding H₂O₂.

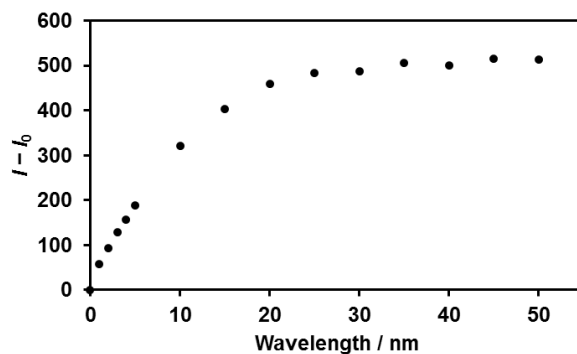


Fig. S10. A plot of a change in fluorescence intensity of **1** (10 μM) in the presence of Zn(OAc)₂ (30 μM) as a function of H₂O₂ concentration added in EtOH at 25 °C. The data were acquired in 30 min after adding H₂O₂. λ_{ex} = 564 nm.

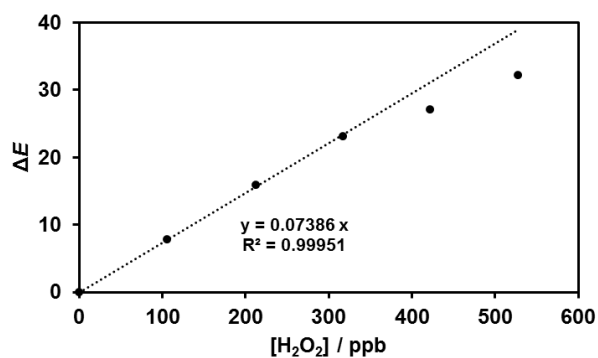


Fig. S11. Colorimetric response of **1** and Zn²⁺-coated filter paper exposed to varying amounts of H₂O₂ vapor. ΔE values were determined using an image-processing program. The dotted line in the graph represents the regression line obtained from dynamic range of the titration curve.

The H₂O₂ vapor detection limit was determined by using relationship between H₂O₂-induced color difference (ΔE) and H₂O₂ concentration (ppb) where ΔE values were acquired using an image processing program. Standard deviation (σ) of the blank measurements were determined from five individual samples to be 1.804. The regression line was obtained in dynamic range of the titration curve (**Fig. S11**), indicating 0.07386 as a slope (m). The detection limit was then calculated from $3\sigma/m$ to be 73.3 ppb.

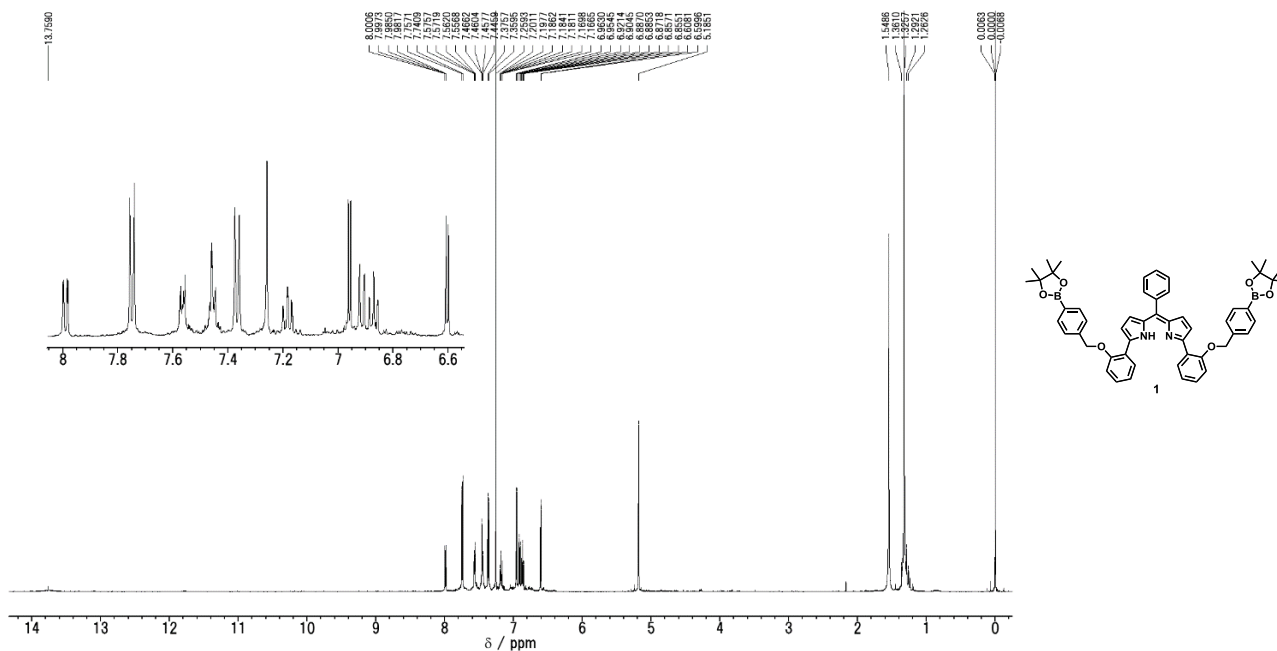


Fig. S12. ¹H NMR spectrum of **1** in CDCl₃.

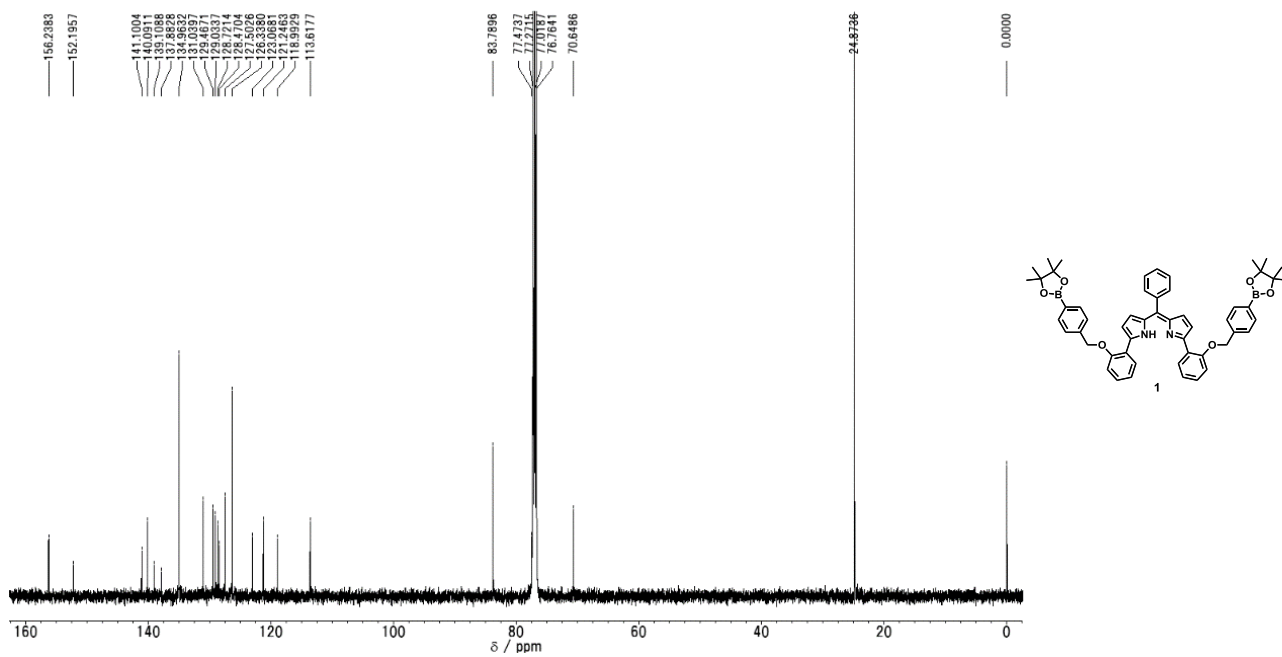


Fig. S13. ^{13}C NMR spectrum of **1** in CDCl_3 .

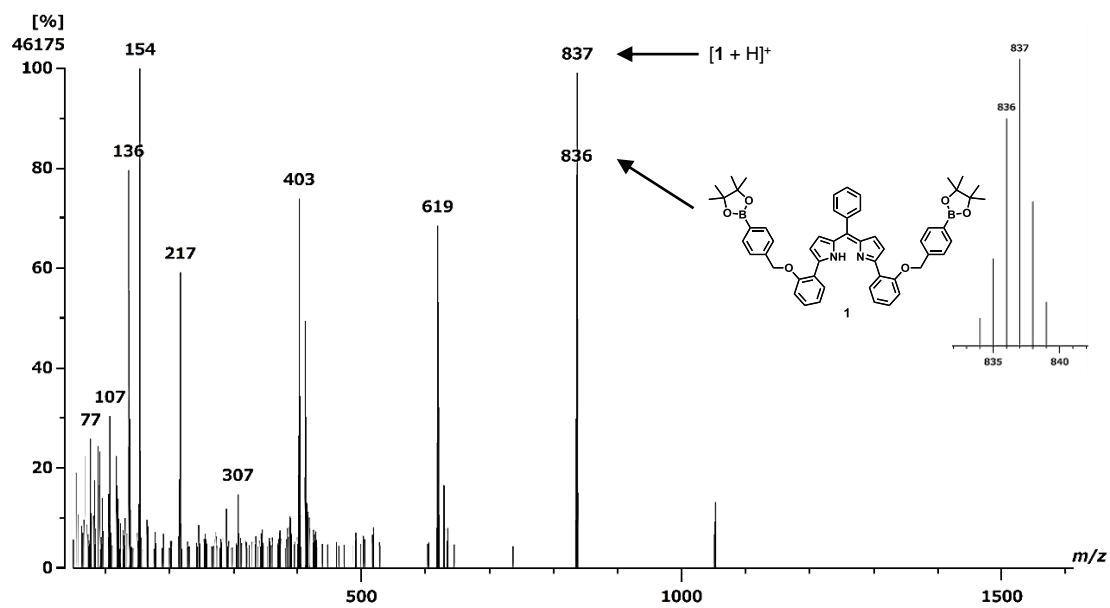


Fig. S14. FAB-MS spectrum in the positive mode of **1**.